Pathology & Oncology Research (2020) 26:967–976
https://doi.org/10.1007/s12253-019-00651-y

ORIGINAL ARTICLE

Identification and Verification of Two Novel Differentially Expressed Proteins from Non-neoplastic Mucosa and Colorectal Carcinoma Via iTRAQ Combined with Liquid Chromatography-Mass Spectrometry

Yuru Bai[1,2] · Jiabao Wang[1] · Zhihua Gao[1] · Erqing Dai[1]

Received: 5 November 2018 / Accepted: 20 March 2019 / Published online: 29 March 2019

Abstract
Recurrence or metastasis of colorectal cancer (CRC) is common following surgery and/or adjuvant therapy, particularly in patients with an advanced stage of the cancer. Identifying key molecular markers of CRC is beneficial for early diagnosis and early treatment, which may eventually improve the prognosis of patients with CRC. Isobaric mass tags for relative and absolute quantification (iTRAQ) in combination with multidimensional liquid chromatography and tandem mass spectrometry (LC-MS/MS) were used to identify differentially expressed proteins between CRC tissues and paired adjacent normal mucosa. Among the 105 patients, adenocarcinoma was the most common CRC subtype, stage III was the most common Tumor-Node-Metastasis stage and high levels of Ki-67 indicated the rapid proliferation of tumor cells in the samples. The LC-MS/MS-based iTRAQ technology identified 271 differentially expressed proteins, with 130 upregulated proteins and 141 downregulated proteins. Bioinformatics analysis revealed that golgin subfamily A member 2 (GOLGA2) and heterogeneous nuclear ribonucleoprotein D0 (hnRNPD) were located in the center of the upregulated protein network, and were closely associated with the development of CRC. The upregulation of GOLGA2 and hnRNPD was further verified in human tissues using western blotting and immunohistochemistry. GOLGA2 and hnRNPD were identified as two novels differentially expressed proteins in human CRC. Furthermore, the LC-MS/MS-based iTRAQ proteomic approach is a useful tool for searching and identifying differentially expressed proteins, and may be used to provide a comprehensive understanding of the processes that mediate the development of CRC.

Keywords Proteomics · Colorectal cancer · Isobaric mass tags for relative and absolute quantification · Multidimensional liquid chromatography and tandem mass spectrometry · Differential expressed proteins

Introduction

Colorectal cancer (CRC) is the third most common malignant cancer according to the incidence and mortality rates [1]. Approximately 694,000 patients succumb to mortality from CRC every year [2]. The incidence rate in developed countries is 8–15%, which is nearly two-fold higher compared with that in developing countries [3]. For patients with stage III and high-risk stage II forms of the cancer, the standard treatment is surgical resection and postoperative adjuvant chemotherapy [4]. However, surgery and chemotherapy are unable to prevent recurrence or metastasis of the disease. Stage T4 cancer, poorly differentiated tissue, intestinal perforation and intestinal obstruction are high-risk factors for disease metastasis and recurrence [5]. As tumor behavior is determined by molecular mechanisms and oncogenic changes in cellular processes, identifying key molecular markers is beneficial for early diagnosis and treatment, which may eventually improve the prognosis of patients with CRC [6]. Numerous CRC-associated molecules and pathways have been reported, including the protein kinase B (Akt) and extracellular signal-regulated kinase 1/2 pathway, the phosphoinositide 3-kinase/Akt/nuclear factor-κB pathway and

✉ Erqing Dai
erqingdai@163.com

[1] Department of Military Medical and Health Care, Characteristic Medical Center of Chinese People's Armed Police Forces, Tianjin 300162, People's Republic of China

[2] Department of Oncology, Nanjing Jiangning Hospital of Traditional Chinese Medicine, Nanjing, Jiangsu 211100, People's Republic of China

Table 1 Parameters for mass spectrometry data analysis

Item	Value
Enzyme	Trypsin
Max Missed Cleavages	2
Fixed modification	Carbamidomethyl (C), iTRAQ4/8plex (N-term), iTRAQ4/8plex(K)
Variable modifications	Oxidation (M), iTRAQ4/8plex (Y)
Peptide Mass Tolerance	±20 ppm
Fragment Mass Tolerance	0.1 Da
Database	Uniprot_HOMO_154578_20160822.fasta
Database pattern	Target-Decoy
Peptide false discovery rate	≤0.01
Peak integration	Integration Window Tolerance: 20 ppm Integration Method: Most Confident Centroid
Scan Event Filters	Mass Analyzer: FTMS MS Order: MS2 Activation Type: HCD
Protein Quantification	Protein ratios calculated as the median of only unique peptides of the protein
Experimental Bias	Normalizes all peptide ratios by the median protein ratio. Median protein ratio should be 1 following normalization

iTRAQ isobaric mass tags for relative and absolute quantification, *HCD* higher-energy collisional dissociation

the Wnt/β-catenin pathway, endothelin receptor A-induced Yes-associated protein/transcriptional coactivator with PDZ-binding motif activation [7–10].

High-throughput proteomics studies may provide a comprehensive understanding of the processes of disease development, and tissue, organ and cell metabolism at the protein level. Quantitative proteomics using cancer and normal tissues have been used to search and identify biomarkers for diagnosis and prognosis for various cancer types [11–15]. Isobaric mass tags for relative and absolute quantification (iTRAQ) in combination with multidimensional liquid chromatography and tandem mass spectrometry enables relative and absolute quantification of multiple samples simultaneously [11, 12]. The present study aimed to identify differentially expressed proteins of non-neoplastic mucosa and colorectal carcinoma based on iTRAQ combined with multidimensional liquid chromatography and tandem mass spectrometry (LC-MS/MS). The results may provide novel insight in the diagnosis and treatment of human CRC.

Table 2 Clinical characteristics of patients with colorectal cancer

Item	Colon cancer (81 cases)	Rectal cancer (24 cases)
Sex (*n*, %)		
Male	46 (56.8)	12 (50)
Female	35 (43.2)	12 (50)
Age (*n*, %)		
20–39	1 (1.2)	1 (4.2)
40–59	31 (38.3)	9 (37.5)
60–85	49 (60.5)	14 (58.3)
Histological type (*n*, %)		
G1	13 (16.0)	5 (20.8)
G2	44 (54.3)	15 (62.5)
G3	15 (18.5)	2 (8.3)
Mucinous	7 (8.6)	2 (8.3)
Signet-ring	2 (2.5)	0 (0)
Tumor-Node-Metastasis stage (*n*, %)		
I	11 (13.6)	3 (12.5)
IIA	27 (33.3)	6 (25)
IIB	1 (1.2)	0 (0)
IIIA	3 (3.7)	3 (12.5)
IIIB	27 (33.3)	8 (33.3)
IIIC	5 (6.2)	2 (8.3)
IVA	5 (6.2)	2 (8.3)
IVB	2 (2.5)	0 (0)
Ki-67 (*n*, %)		
Grade I	10 (12.3)	3 (12.5)
Grade II	27 (33.3)	11 (45.8)
Grade III	44 (54.3)	10 (41.7)
Smoking (*n*, %)		
Yes	32 (39.5)	8 (33.3)
No	49 (60.5)	16 (66.7)
Drinking (*n*, %)		
Yes	15 (18.5)	6 (25)
No	66 (81.5)	18 (75)

Materials and Methods

Patients Between February 2015 and September 2016, 105 patients (aged from 18 to 85 years old; 58 males and 47 females) with CRC treated at the Affiliated Hospital of Logistics University of Chinese People's Armed Police Forces (CAPF; Tianjin, China) were recruited for the study. The patients all received surgical resection and didn't received any treatment before the surgery. The study was ethically approved by the Ethics Committee of the Affiliated Hospital of Logistics College of CAPF. Written informed consent was obtained from all patients. All patients underwent colorectal surgery and the collected tissues were examined pathologically, following a standard protocol. Tumor classification was applied according to the TNM staging revised by the International Union Against Cancer (UICC) (https://www.uicc.org/). Tumors were staged in accordance with the tumor-node-metastasis (TNM) clinicopathological staging system.

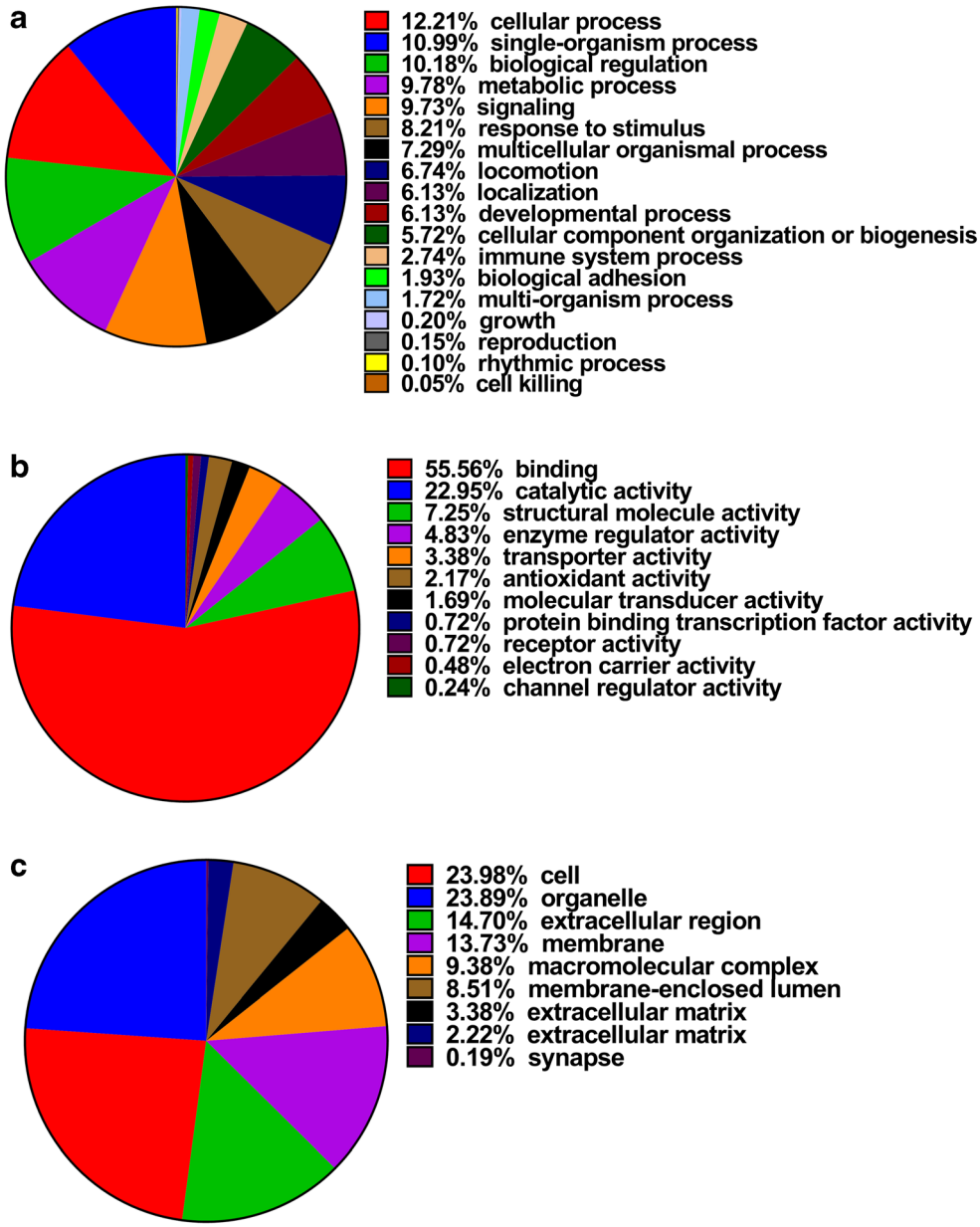

Fig. 1 Gene ontology enrichment analysis of differentially expressed proteins between colorectal cancer tumor tissues and paired non-tumorous mucosa. **a** Biological process. **b** Molecular function. **c** cellular component

Tissue Samples Paired tissue samples were obtained from each patient. Adjacent mucosa samples >10 cm from the tumor margins were obtained and regarded as normal tissues. Following washing twice with phosphate-buffered saline, the CRC tumor tissues and paired adjacent normal tissues were immediately stored in nitrogen vapor at −170 °C.

Protein Digestion and iTRAQ Labeling CRC tissue samples and paired adjacent normal tissues were thawed and suspended in 1 ml ice cold SDT lysis buffer (4%SDS, 100 mM Tris-HCl, 1 mM DTT, pH = 7.6) in a 2 ml centrifuge tube with quartz sand and 1/4 in. ceramic beads (cat no. MP6540–424; MP Biomedicals, LLC, Santa Ana, CA, USA). The protein concentrations were measured using a Bradford-type assay (Beyotime Institute of Biotechnology, Haimen, China) according to the manufacturer's protocol.. Subsequently, ~100 mg protein from each sample was reduced, alkylated and processed using trypsin at 37 °C for 17 h. The peptide segments were desalted using a C18 cartridge, and freeze-dried with the addition of 40 μl dissolution buffer in the iTRAQ Reagent-Multiplex Buffer kit (Applied Biosystems; Thermo Fisher Scientific, Inc.) according to the manufacturer's protocol.

High-Performance Liquid Chromatography (HPLC) The labeled peptides were mixed and fractionated by strong cation-exchange chromatography using an AKTA Purifier 100 (GE Healthcare, Boston, USA). Buffer A (10 mM KH2PO4, 25%ACN, pH = 3.0) and buffer B (10 mM KH2PO4 ,

500 mM KCL , 25%ACN , pH = 3.0) were used. The strong cation exchange (300SCX) column (Agilent, California, USA) was equilibrated with solution A and the sample was loaded from the injector to the column for a flow rate of 1 mL/min. The linear gradient was determined by the project proposal: 0% buffer B for 25 min; 0–10% buffer B at 25–30 min; 10–20% buffer B at 32–42 min; 20–45% buffer B at 42–47 min; 45–100% buffer B at 47–52 min; hold on 100% buffer B for 1 h, then adjusted the buffer B to 0%. The absorbance at 214 nm was monitored during the elution process, and the eluted fractions were collected every 1 min. The fractions were freeze-dried and were desalted using a C18 cartridge.

Liquid Chromatograph-Mass Spectrometer/ Mass Spectrometer (LC-MS/MS) Each sample was separated using an Easy nLC 1200 system (Thermo Fischer Scientific, Waltham, MA, USA). Buffer A (0.1% formic acid) and buffer B (84% acetonitrile). The sample was loaded from the autosampler to the loading column (Thermo Scientific Acclaim PepMap100, 100 μm*2 cm, nanoViper C18), and separated through an analytical column (Thermo scientific EASY column, 10 cm, ID 75 μm, 3 μm, C18-A2) at a flow rate of 300 nl/min. The linear gradient was determined by the project proposal: 0–35% buffer B for 50 min; 35–100% buffer B at 50–55 min; hold on 100% buffer B at 55–60 min.

The sample was chromatographed and subjected to mass spectrometry using a Q-Exactive mass spectrometer (Thermo). The analysis time was 240 min, the detection mode was positive ion, the parent ion scanning range was 300-1800 m/z, the primary mass spectrometer resolution was 70,000 at 200 m/z, the Automatic gain control (AGC) target was 1e6, and the Maximum IT was 50 ms. The Dynamic exclusion was 60.0 s. The mass-to-charge ratio of the polypeptide and polypeptide fragments was collected as follows: 20 fragments were acquired after each full scan, the MS2 Activation Type was HCD, and the Isolation window was 2 m/z. 17,500 at 200 m/z, Normalized Collision Energy is 30 eV and Underfill is 0.1%.

Data were analyzed using Mascot 2.2 (www.matrixscience.com) and Proteome Discoverer 1.4 software (www.pdfdrive.com). Data were searched based on the parameters presented in Table 1.

Bioinformatics Analysis Gene Ontology (GO) annotations were performed as previous reference [16]. The process of GO annotations can be roughly divided into sequence alignment (Blast), GO (Mapping), GO from entry notes (Annotation) and complement (Annotation Augmentation) notes using Blast2GO in setting the target protein annotation. Using the WebGestalt tool [17], GO enrichment analyses were performed by uploading differentially expressed proteins and comparing with all proteins from the known human proteome [18].

Kyoto Encyclopedia of Genes and Genomes (KEGG) pathway enrichment annotations were used to analyze the differentially expressed proteins, and orthologous genes and their products with similar functions within the same pathway were classified as a group [19, 20]. In the present study, KEGG Automatic Annotation Sever (KAAS) software was used to analyze the target proteins and map the pathways involved in tumorigenesis [20].

A protein-protein interaction network for differentially expressed proteins was created using Cytoscape (3.5.0) following searching the IntAct database [21, 22].

Western Blot Analysis Cells were lysed by RIPA lysis buffer (Thermo). Protein (60 μg) was separated using 12% SDS-PAGE. The primary antibodies used were golgin subfamily A member 2 (GOLGA2) antibody (dilution, 1:1000; ProteinTech Group, Inc., Chicago, IL, USA) and anti-heterogeneous nuclear ribonucleoprotein D0 (hnRNPD) antibody (dilution, 1:500; ProteinTech Group, Inc.). Subsequent to incubation for 2 h, the membranes were washed three times using Tris-buffered saline with 0.5% Tween-20 (TBST) for 5 min each time. Subsequently, the membranes were incubated with secondary antibodies for 1 h at room temperature, followed by four washes in TBST for 10 min per wash. The membranes were developed using ECL Western Blotting Detection Reagent (GE Healthcare Life Sciences, Little Chalfont, UK) and analyzed using Amersham Imager 600 (GE Healthcare, Chicago, IL, USA).

Immunohistochemistry (IHC) CRC tissues and paired non-neoplastic mucosa were fixed in 10% formalin for 48 h. Embedded the samples in paraffin and sectioned in 4-μm thickness. High pressure heat repair was used for antigen retrieval. The thicknesses were incubated in 3% H_2O_2 for 10 min to eliminate endogenous peroxidase activity. Incubated the thicknesses with primary antibodies (anti-GOLGA2, 1:2000, Cell Signaling, Danvers, MA, USA; anti-hnRNPD, 1:2000, Cell Signaling) at room temperature for 1 h, followed by incubating with secondary antibodies (1:10000, Cell Signaling). Stained the thicknesses with DAB (Sigma-Aldrich, Missouri, USA) for 5 min, then stained with haematoxylin for 1 min. Finally, the images were observed with a microscope (LEICADMLB2, Germany).

Fig. 2 KEGG pathway enrichment analysis of the 271 identified differentially expressed proteins between colorectal cancer tumor tissues and paired non-tumorous mucosa. **a** Top 20 KEGG pathways. **b** Enriched KEGG pathways. VSMC, vascular smooth muscle contraction; AC, actin cytoskeleton; DM, drug metabolism; CYP450, cytochrome P450; cGMP, cyclic guanosine monophosphate; cAMP, cyclic denosine monophosphate; ECM, extracellular matrix; SP, signaling pathway; PDA, protein digestion and absorption; VI, virus infection; KEGG, Kyoto Encyclopedia of Genes and Genomes

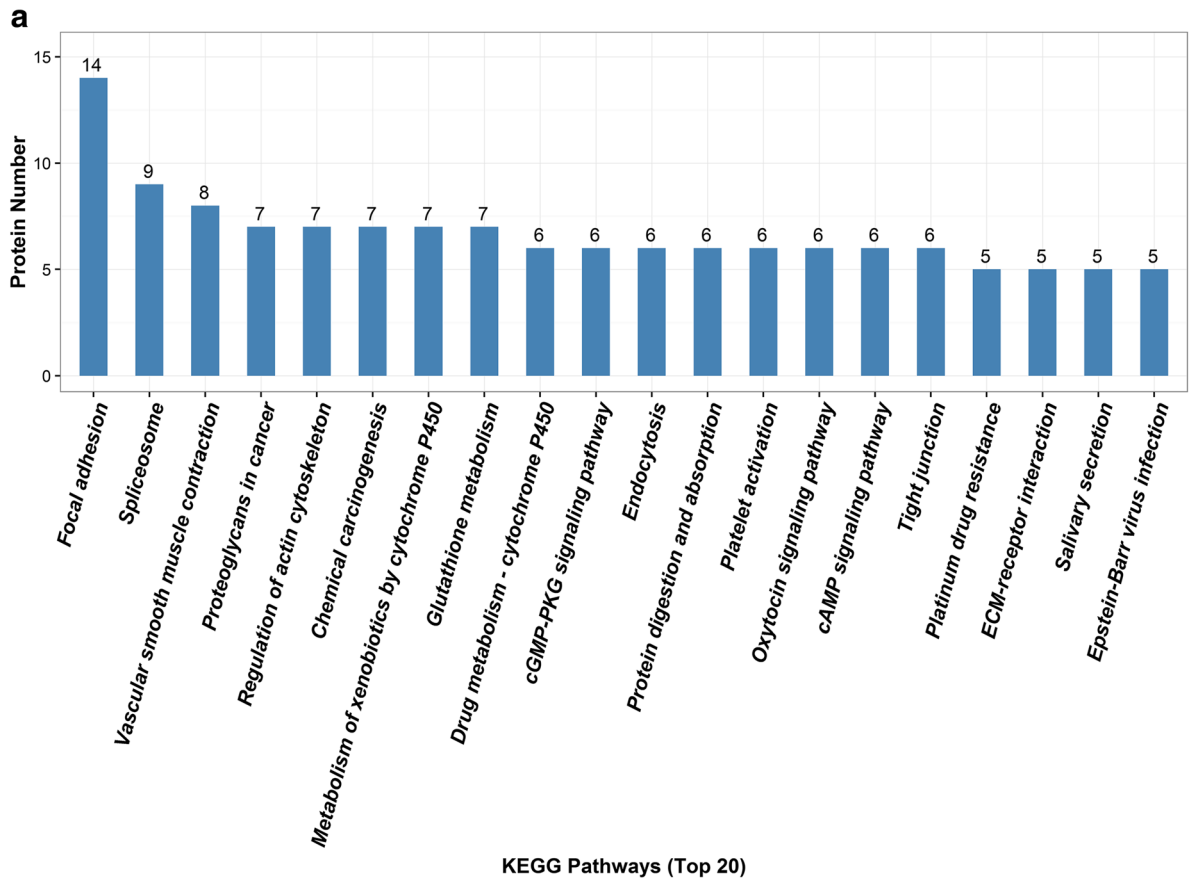
a
Protein Number
15
10
5
0
14
9
8
7
7
7
7
7
6
6
6
6
6
6
6
6
5
5
5
5
Focal adhesion
Spliceosome
Vascular smooth muscle contraction
Proteoglycans in cancer
Regulation of actin cytoskeleton
Chemical carcinogenesis
Metabolism of xenobiotics by cytochrome P450
Glutathione metabolism
Drug metabolism - cytochrome P450
cGMP-PKG signaling pathway
Endocytosis
Protein digestion and absorption
Platelet activation
Oxytocin signaling pathway
cAMP signaling pathway
Tight junction
Platinum drug resistance
ECM-receptor interaction
Salivary secretion
Epstein-Barr virus infection
KEGG Pathways (Top 20)

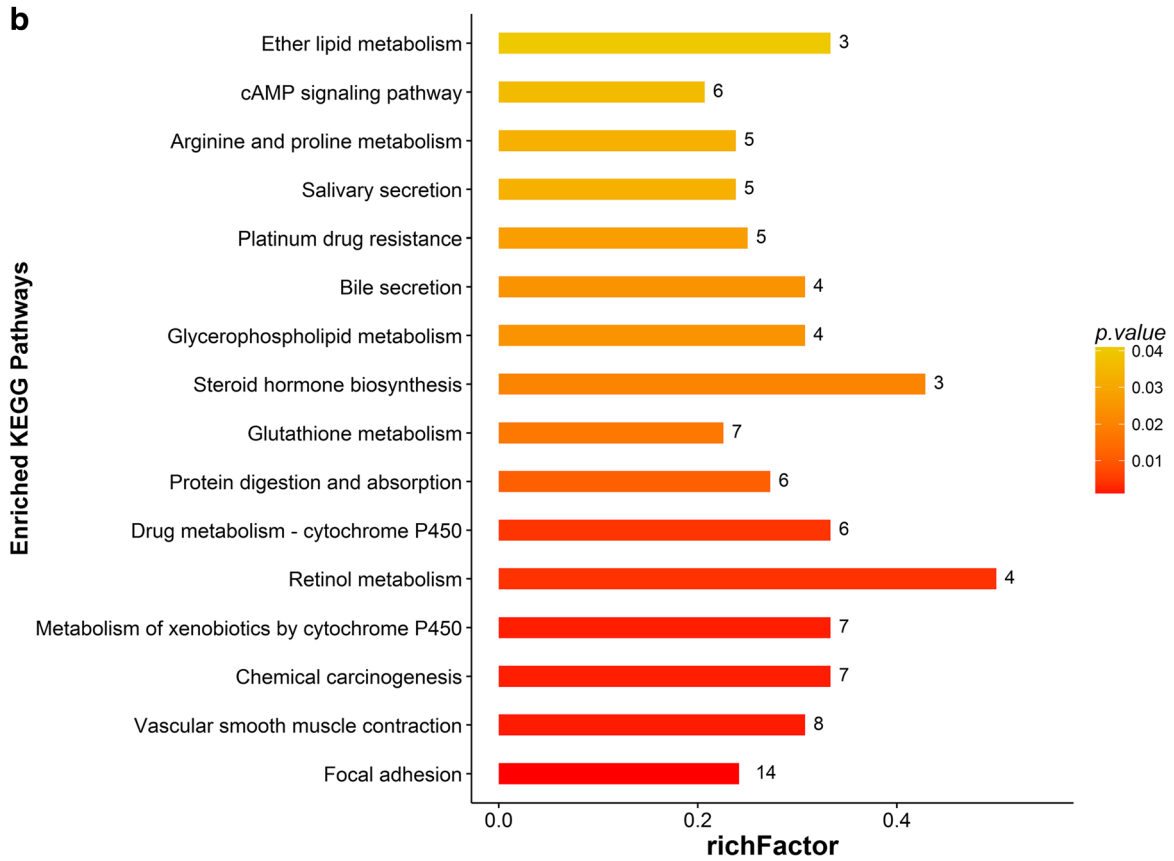
b
Enriched KEGG Pathways
Ether lipid metabolism
cAMP signaling pathway
Arginine and proline metabolism
Salivary secretion
Platinum drug resistance
Bile secretion
Glycerophospholipid metabolism
Steroid hormone biosynthesis
Glutathione metabolism
Protein digestion and absorption
Drug metabolism - cytochrome P450
Retinol metabolism
Metabolism of xenobiotics by cytochrome P450
Chemical carcinogenesis
Vascular smooth muscle contraction
Focal adhesion
3
6
5
5
5
4
4
3
7
6
6
4
7
7
8
14
0.0
0.2
0.4
richFactor
p.value
0.04
0.03
0.02
0.01

Results

Clinical Characteristics of Patients with CRC The clinical characteristics of the 105 patients with CRC are presented in Table 2. There were 81 cases (77%) of colon cancer and 24 cases (23%) of rectal cancer. Among the 105 patients, adenocarcinoma was highly prevalent, TNM staging was primarily stage III and high levels of Ki-67 expression indicated the rapid proliferation of tumor cells. The number of patients with smoking and drinking habits was relatively small (Table 2).

LC-MS/MS-Based iTRAQ iTRAQ-MS was used to identify the differentially expressed proteins between CRC tumor tissues and their paired non-tumorous mucosa. In total, 271 differentially expressed proteins were identified by the LC-MS/MS-based iTRAQ technology, with 130 upregulated proteins and 141 downregulated proteins.

GO Enrichment Analysis The differentially expressed proteins were further classified according to the biological process (BP), molecular function (MF) and cellular compartment (CC) domains using GO term analysis. In the biological process domain, the majority of proteins were involved in 'cellular processes', 'single-organism processes', 'biological regulation', 'metabolic processes', 'response to stimulus' and 'developmental processes' (Fig. 1a). For molecular function, the majority of proteins were associated with 'binding', 'catalytic activity', 'structural molecule activity' and 'enzyme regulator activity' (Fig. 1b). The majority of the differentially expressed proteins were located at specific subcellular compartments, which are associated with cellular function. The compartments may be roughly divided into the following categories: 'cell', 'organelle', 'extracellular region', 'membrane', 'macromolecular complex' and 'membrane-enclosed lumen' (Fig. 1c). These results indicated that the differentially expressed proteins are associated with various biological processes and molecular functions.

KEGG Pathway Enrichment Analysis The pathways involved in CRC tumorigenesis were identified through KEGG enrichment analysis. The analysis identified 16 pathways that were associated with CRC, as presented in Fig. 2. The association between the 217 differentially expressed proteins was further analyzed using the IntAct database. A protein-protein interaction diagram generated using Cytoscape software. The results revealed that among all upregulated proteins, GOLGA2 and hnRNPD were at the center of the network. Another 130 upregulated proteins were selected for further analysis of protein-protein interactions, as downregulated proteins may not be suitable as potential biomarkers, as previously reported [23]. The results revealed GOLGA2 and hnRNPD at the center of the upregulated-protein network, and these proteins were closely associated with the development of the CRC according to the bioinformatics analysis (Fig. 3).

Verification of GOLGA2 and hnRNPD Expression of iTRAQ Analysis In the up-regulated central network diagram, GOLGA2 and hnRNPD were at the key points of the network. Furthermore, GOLGA2 and hnRNPD were closely related to the occurrence and development of tumors according to the bioinformatics analysis of proteins. Therefore, we conducted further research on GOLGA2 and hnRNPD through western blot and immunohistochemistry assays. As presented in Fig. 4, the expression of GOLGA2 and hnRNPD in CRC tissues were higher compared with those in the paired normal mucosa. Further verification of the two representative proteins identified by iTRAQ analysis was performed using immunohistochemistry, which produced similar results, with an increase in the expression of GOLGA2 and hnRNPD in CRC tissues as compared with non-neoplastic mucosa (Fig. 5). Furthermore, different expressed patterns of GOLGA2 and hnRNPD were observed by IHC. GOLGA2 was exclusively expressed in tumor-associated stromal mesenchymal cells, while hnRNPD was predominantly expressed in the neoplastic epithelial cells (Fig. 5).

Discussion

In the present study, 105 patients with CRC were recruited. Based on the analysis of clinical data, it was observed that colon cancer was more common in patients >40 years of age and that the most common TNM stage was stage III. The results suggested that it is difficult to identify CRC at an early stage, and the majority of the patients were not treated until the disease had progressed to advanced stages. Thus, developing methods for the early detection and diagnosis of CRC are of great importance.

The development of quantitative proteomic techniques based on iTRAQ provides another method for identifying differentially expressed proteins involved in the development of CRC. In the present study, iTRAQ combined with LC-MS/MS was used to compare protein expression in CRC tissues and adjacent normal tissues. The analysis identified 271 differential proteins, and 2 differential proteins (GOLGA2 and hnRNPD) were selected for further validation. GOLGA2 and hnRNPD were upregulated in CRC tissue, as compared with adjacent normal mucosa, suggesting that GOLGA2 and hnRNPD may be potential biomarkers for CRC.

The Golgi apparatus is a central organelle in the cell secretory pathway involved in the processing of secreted proteins and post-translational modifications of endoplasmic reticulum (ER) transmembrane proteins. In protein processing pathways, the Golgi apparatus is the connection between the ER and endosomes, lysosomes and plasma membranes [24, 25].

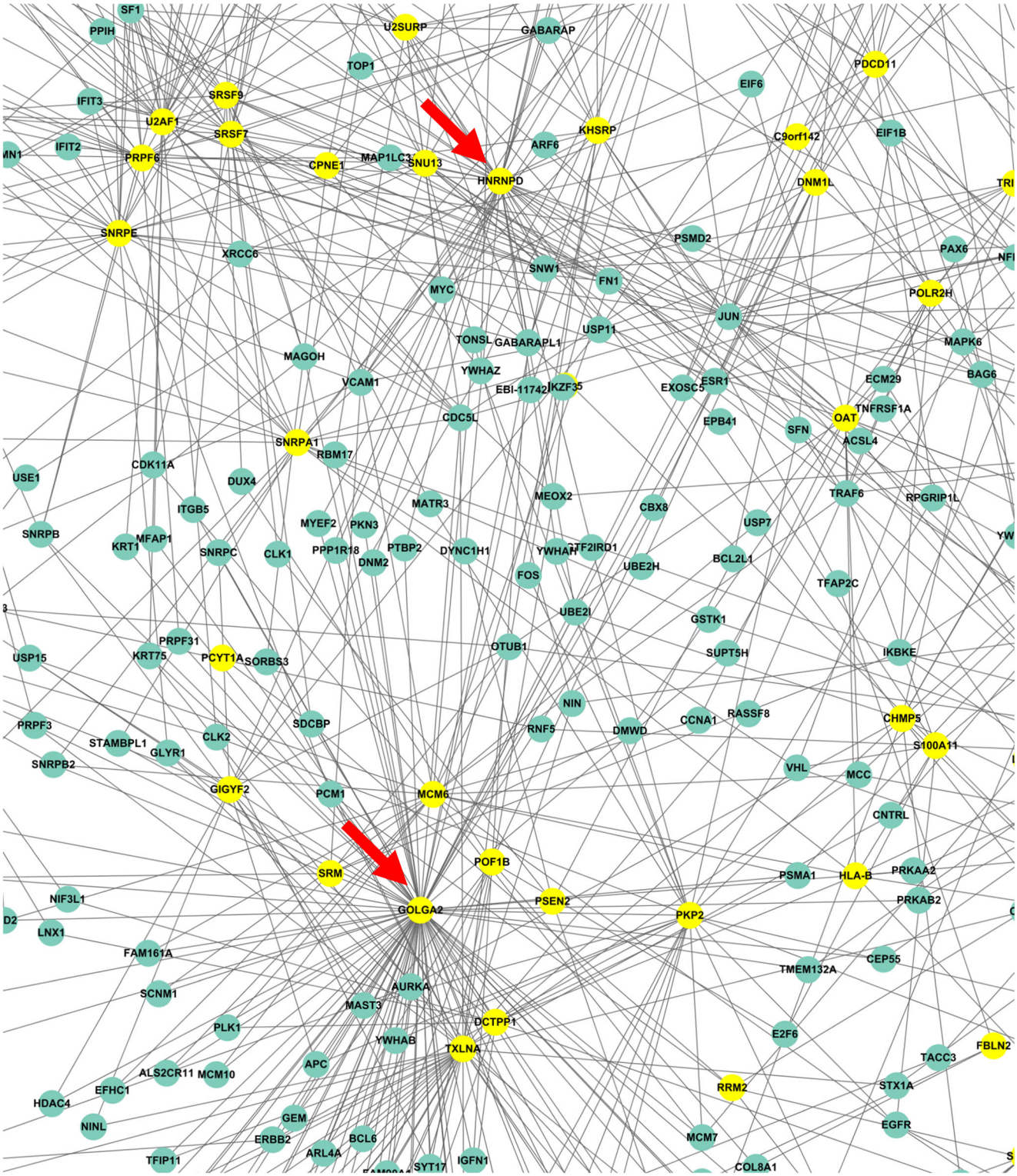

Fig. 3 Protein-protein interactions among 130 upregulated differentially expressed proteins between colorectal cancer tumor tissues and paired non-tumorous mucosa

Previously, the ER, the Golgi apparatus and lysosomes have been considered as novel targets for cancer treatment [26].

GOLGA2 is a cis Golgi protein that is separated from the detergent and salt-tolerant Golgi body. It serves an important role in maintaining Golgi structure and Golgi accumulation. Additionally, GOLGA2 is involved in ER-Golgi transport, glycosylation and in cell cycle progression. However, a number of studies have reported that GOLGA2 has an unexpected role in

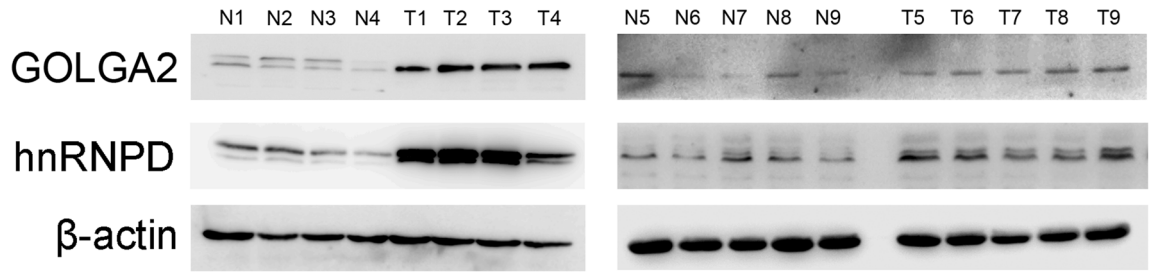

Fig. 4 Protein expression of GOLGA2 and hnRNPD between colorectal cancer tumor tissues and paired non-tumorous mucosa. The expression of GOLGA2 and hnRNPD were determined by western blot analysis. N, non-tumorous tissues; T, tumorous tissues; GOLGA2, golgin subfamily A member 2; hnRNPD, heterogeneous nuclear ribonucleoprotein D0

various cellular processes in diseases, including cell division, polarization and directed cell migration. Recent reports have revealed that the downregulation of GOLGA2 inhibits protein transport between ER and the Golgi apparatus, and induces autophagy [26, 27]. Autophagy contributes to tumor suppression, and autophagy defects are associated with tumor progression [26, 27]. The upregulation of GOLGA2 results in reduced E-cadherin expression; and the downregulation of E-cadherin expression has a key role in epithelial-mesenchymal transition (EMT) [28] associated with a loss of cell polarity [29–31].

EMT is a major pathogenic feature of CRC, which involves tumor cell migration, invasion and proliferation [32]. The establishment and maintenance of cell polarity is an important feature of the majority of epithelial cells. Polar mechanisms are essential for normal cell function to maintain homeostasis in cells and tissues, and polar changes may result in the loss of differentiation and tumor progression [30, 33]. The present study revealed that GOLGA2 expression was enhanced in CRC tissues compared with paired normal mucosa. GOLGA2 has been reported to be highly expressed in cervical cancer cell lines, lung cancer cells and gastric cancer cells [26, 34, 35]. To the best of our knowledge, this is the first report of increased GOLGA2 expression in human CRC.

hnRNPs are a major group of nuclear proteins. These proteins are mainly involved in RNA splicing, interaction with telomeres, DNA repair, cell signal transduction and protein translation [36]. hnRNPs also have numerous other potential effects in the inhibition of angiogenesis, apoptosis, invasion and EMT [36]. A variety of studies have reported that the overexpression of hnRNPs result in tumor progression, including in esophageal cancer, oral cancer and gastric cancer [37–39]. hnRNPs may enhance the expression of c-myc, c-fos and c-jun, and regulate the proliferation of hepatoma cells in transgenic mice [23]. In thyroid cancer, cytoplasmic hnRNPD may be recruited to disrupt the stability of mRNA encoding cyclin-dependent kinase inhibitors, resulting in uncontrolled growth and development of tumor cells [40]. Other studies have reported that hnRNPK is involved in the promotion of CRC cell growth and metastasis, and that the upregulation of hnRNPK reduces CRC radiosensitivity [41, 42]. In the present study, the upregulation of hnRNPD in human CRC compared with adjacent non-neoplastic mucosa was identified using

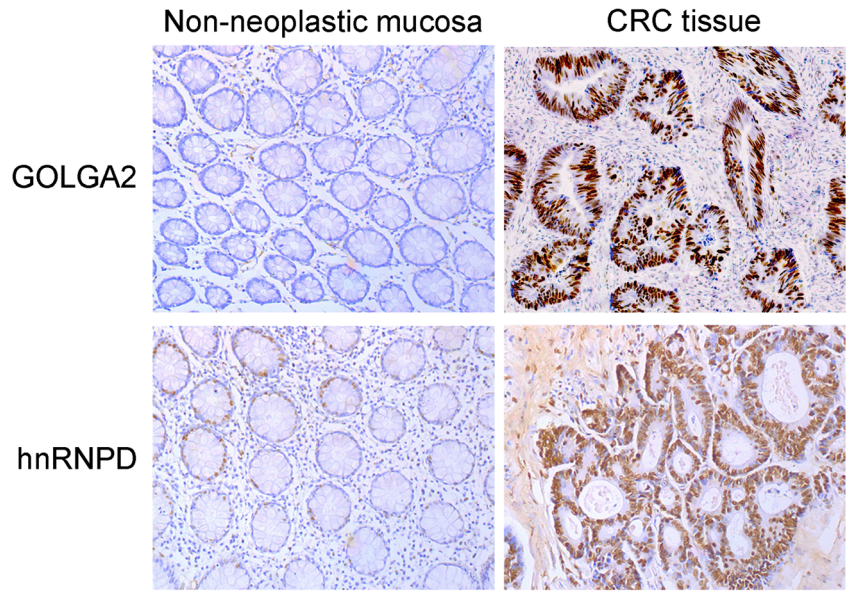

Fig. 5 Immunohistochemistry analysis of GOLGA2 and hnRNPD expression in non-neoplastic mucosa and CRC tissues. GOLGA2 was expressed in tumor-associated stromal mesenchymal cells (upper right). hnRNPD was expressed in the neoplastic epithelial cells (bottom right). Original magnification, ×200. CRC, colorectal cancer; GOLGA2, golgin subfamily A member 2; hnRNPD, heterogeneous nuclear ribonucleoprotein D0

iTRAQ and LC-MS, and validated by western blotting and immunohistochemistry.

In conclusion, GOLGA2 and hnRNPD were identified as two novel differentially expressed proteins in human CRC. An LC-MS/MS-based iTRAQ proteomic approach was identified to be a useful tool in searching and identifying differentially expressed proteins in CRC, and may provide a comprehensive understanding of the processes involved in the development of CRC.

Funding The present study was supported by the National Natural Science Foundation of China (grant no.81273745), the Tianjin Natural Science Foundation (grant no.11JCYBJC10900), Sub Project of Key Projects in Tianjin (grant no.15ZXLCSY00040-08) and Science and Technology Program of Tianjin, China (grant no.16ZXHLSY00120).

Compliance with Ethical Standards

Competing Interests The authors declare that they have no competing interests.

References

1. Ferlay J, Soerjomataram I, Dikshit R, Eser S, Mathers C, Rebelo M, Parkin DM, Forman D, Bray F (2015) Cancer incidence and mortality worldwide: sources, methods and major patterns in GLOBOCAN 2012. Int J Cancer 136(5):E359–E386
2. Karanikas M, Esebidis A (2016) Increasing incidence of colon cancer in patients <50 years old: a new entity? Ann Transl Med 4(9):164
3. Torre LA, Bray F, Siegel RL, Ferlay J, Lortet-Tieulent J, Jemal A (2015) Global cancer statistics, 2012. CA Cancer J Clin 65(2):87–108
4. Barton MK (2012) Oxaliplatin in the adjuvant treatment of colon cancer. CA Cancer J Clin 62(1):3–4
5. Lote H, Spiteri I, Ermini L, Vatsiou A, Roy A, McDonald A, Maka N, Balsitis M, Bose N, Simbolo M, Mafficini A, Lampis A, Hahne JC, Trevisani F, Eltahir Z, Mentrasti G, Findlay C, Kalkman EAJ, Punta M, Werner B, Lise S, Aktipis A, Maley C, Greaves M, Braconi C, White J, Fassan M, Scarpa A, Sottoriva A, Valeri N (2017) Carbon dating cancer: defining the chronology of metastatic progression in colorectal cancer. Ann Oncol 28:1243–1249
6. Chaffer CL, Weinberg RA (2011) A perspective on cancer cell metastasis. Science 331(6024):1559–1564
7. Tao Y, Han T, Zhang T, Sun C (2017) Sulfatase-2 promotes the growth and metastasis of colorectal cancer by activating Akt and Erk1/2 pathways. Biomed Pharmacother 89:1370–1377
8. Shen T, Yang Z, Cheng X, Xiao Y, Yu K, Cai X, Xia C, Li Y (2017) CXCL8 induces epithelial-mesenchymal transition in colon cancer cells via the PI3K/Akt/NF-kappaB signaling pathway. Oncol Rep 37:2095–2100
9. Huang GL et al (2017) Oncogenic retinoic acid receptor gamma knockdown reverses multi-drug resistance of human colorectal cancer via Wnt/beta-catenin pathway. Cell Cycle:1–8
10. Wang Z et al (2017) Endothelin promotes colorectal tumorigenesis by activating YAP/TAZ. Cancer Res 77(9):2413–2423
11. Chen CL, Chung T, Wu CC, Ng KF, Yu JS, Tsai CH, Chang YS, Liang Y, Tsui KH, Chen YT (2015) Comparative tissue proteomics of microdissected specimens reveals novel candidate biomarkers of bladder Cancer. Mol Cell Proteomics 14(9):2466–2478
12. Bouchal P, Roumeliotis T, Hrstka R, Nenutil R, Vojtesek B, Garbis SD (2009) Biomarker discovery in low-grade breast cancer using isobaric stable isotope tags and two-dimensional liquid chromatography-tandem mass spectrometry (iTRAQ-2DLC-MS/MS) based quantitative proteomic analysis. J Proteome Res 8(1):362–373
13. Chen RX, Song HY, Dong YY, Hu C, Zheng QD, Xue TC, Liu XH, Zhang Y, Chen J, Ren ZG, Liu YK, Cui JF (2014) Dynamic expression patterns of differential proteins during early invasion of hepatocellular carcinoma. PLoS One 9(3):e88543
14. Li Y, Wang X, Ao MH, Gabrielson E, Askin F, Zhang H, Li QK (2013) Aberrant Mucin5B expression in lung adenocarcinomas detected by iTRAQ labeling quantitative proteomics and immunohistochemistry. Clin Proteomics 10(1):15
15. Sun CY, Xia GW, Xu K, Ding Q (2010) Application of iTRAQ in proteomic study of prostate cancer. Zhonghua Nan Ke Xue 16(8): 741–744
16. Ashburner M, Ball CA, Blake JA, Botstein D, Butler H, Cherry JM, Davis AP, Dolinski K, Dwight SS, Eppig JT, Harris MA, Hill DP, Issel-Tarver L, Kasarskis A, Lewis S, Matese JC, Richardson JE, Ringwald M, Rubin GM, Sherlock G (2000) Gene ontology: tool for the unification of biology. The gene ontology consortium. Nat Genet 25(1):25–29
17. Zhang B, Kirov S, Snoddy J (2005) WebGestalt: an integrated system for exploring gene sets in various biological contexts. Nucleic Acids Res 33(Web Server issue):W741–W748
18. da Huang W, Sherman BT, Lempicki RA (2009) Systematic and integrative analysis of large gene lists using DAVID bioinformatics resources. Nat Protoc 4(1):44–57
19. Kanehisa M, Furumichi M, Tanabe M, Sato Y, Morishima K (2017) KEGG: new perspectives on genomes, pathways, diseases and drugs. Nucleic Acids Res 45(D1):D353–D361
20. Kanehisa M, Sato Y, Kawashima M, Furumichi M, Tanabe M (2016) KEGG as a reference resource for gene and protein annotation. Nucleic Acids Res 44(D1):D457–D462
21. Orchard S, Ammari M, Aranda B, Breuza L, Briganti L, Broackes-Carter F, Campbell NH, Chavali G, Chen C, del-Toro N, Duesbury M, Dumousseau M, Galeota E, Hinz U, Iannuccelli M, Jagannathan S, Jimenez R, Khadake J, Lagreid A, Licata L, Lovering RC, Meldal B, Melidoni AN, Milagros M, Peluso D, Perfetto L, Porras P, Raghunath A, Ricard-Blum S, Roechert B, Stutz A, Tognolli M, van Roey K, Cesareni G, Hermjakob H (2014) The MIntAct project–IntAct as a common curation platform for 11 molecular interaction databases. Nucleic Acids Res 42(Database issue):D358–D363
22. Shannon P, Markiel A, Ozier O, Baliga NS, Wang JT, Ramage D, Amin N, Schwikowski B, Ideker T (2003) Cytoscape: a software environment for integrated models of biomolecular interaction networks. Genome Res 13(11):2498–2504
23. Dai P, Wang Q, Wang W, Jing R, Wang W, Wang F, Azadzoi K, Yang JH, Yan Z (2016) Unraveling molecular differences of gastric Cancer by label-free quantitative proteomics analysis. Int J Mol Sci 17(1)
24. Witkos TM, Lowe M (2017) Recognition and tethering of transport vesicles at the Golgi apparatus. Curr Opin Cell Biol 47:16–23
25. Potelle S, Klein A, Foulquier F (2015) Golgi post-translational modifications and associated diseases. J Inherit Metab Dis 38(4):741–751
26. Chang SH, Hong SH, Jiang HL, Minai-Tehrani A, Yu KN, Lee JH, Kim JE, Shin JY, Kang B, Park S, Han K, Chae C, Cho MH (2012) GOLGA2/GM130, cis-Golgi matrix protein, is a novel target of anticancer gene therapy. Mol Ther 20(11):2052–2063
27. Nakamura N (2010) Emerging new roles of GM130, a cis-Golgi matrix protein, in higher order cell functions. J Pharmacol Sci 112(3):255–264
28. Medici D, Hay ED, Olsen BR (2008) Snail and slug promote epithelial-mesenchymal transition through beta-catenin-T-cell factor-4-dependent expression of transforming growth factor-beta3. Mol Biol Cell 19(11):4875–4887

29. Tse JC, Kalluri R (2007) Mechanisms of metastasis: epithelial-to-mesenchymal transition and contribution of tumor microenvironment. J Cell Biochem 101(4):816–829
30. Kalluri R, Weinberg RA (2009) The basics of epithelial-mesenchymal transition. J Clin Invest 119(6):1420–1428
31. Godde NJ, Galea RC, Elsum IA, Humbert PO (2010) Cell polarity in motion: redefining mammary tissue organization through EMT and cell polarity transitions. J Mammary Gland Biol Neoplasia 15(2):149–168
32. Lee SC, Kim OH, Lee SK, Kim SJ (2015) IWR-1 inhibits epithelial-mesenchymal transition of colorectal cancer cells through suppressing Wnt/beta-catenin signaling as well as survivin expression. Oncotarget 6(29):27146–27159
33. Nieto MA (2013) Epithelial plasticity: a common theme in embryonic and cancer cells. Science 342(6159):1234850
34. Roy E, Bruyère J, Flamant P, Bigou S, Ausseil J, Vitry S, Heard JM (2012) GM130 gain-of-function induces cell pathology in a model of lysosomal storage disease. Hum Mol Genet 21(7):1481–1495
35. Zhao J, Yang C, Guo S, Wu Y (2015) GM130 regulates epithelial-to-mesenchymal transition and invasion of gastric cancer cells via snail. Int J Clin Exp Pathol 8(9):10784–10791
36. Han N, Li W, Zhang M (2013) The function of the RNA-binding protein hnRNP in cancer metastasis. J Cancer Res Ther 9(Suppl): S129–S134
37. Gouble A, Grazide S, Meggetto F, Mercier P, Delsol G, Morello D (2002) A new player in oncogenesis: AUF1/hnRNPD overexpression leads to tumorigenesis in transgenic mice. Cancer Res 62(5): 1489–1495
38. Geng Y, Zhang L, Xu M, Sheng W, Dong A, Cao J, Cao J (2015) The expression and significance of hnRNPD in esophageal squamous cell carcinoma cells. Xi Bao Yu Fen Zi Mian Yi Xue Za Zhi 31(12):1659–1663
39. Kumar M, Matta A, Masui O, Srivastava G, Kaur J, Thakar A, Shukla NK, RoyChoudhury A, Sharma M, Walfish PG, Michael Siu KW, Chauhan SS, Ralhan R (2015) Nuclear heterogeneous nuclear ribonucleoprotein D is associated with poor prognosis and interactome analysis reveals its novel binding partners in oral cancer. J Transl Med 13:285
40. Trojanowicz B, Brodauf L, Sekulla C, Lorenz K, Finke R, Dralle H, Hoang-Vu C (2009) The role of AUF1 in thyroid carcinoma progression. Endocr Relat Cancer 16(3):857–871
41. Eder S, Arndt A, Lamkowski A, Daskalaki W, Rump A, Priller M, Genze F, Wardelmann E, Port M, Steinestel K (2017) Baseline MAPK signaling activity confers intrinsic radioresistance to KRAS-mutant colorectal carcinoma cells by rapid upregulation of heterogeneous nuclear ribonucleoprotein K (hnRNP K). Cancer Lett 385:160–167
42. Zhang Z, Zhou C, Chang Y, Zhang Z, Hu Y, Zhang F, Lu Y, Zheng L, Zhang W, Li X, Li X (2016) Long non-coding RNA CASC11 interacts with hnRNP-K and activates the WNT/beta-catenin pathway to promote growth and metastasis in colorectal cancer. Cancer Lett 376(1):62–73